Large on-chip Brillouin net amplification in silicon-based nano-photonics

Cite as: AIP Advances **9**, 125032 (2019); https://doi.org/10.1063/1.5125699
Submitted: 25 August 2019 . Accepted: 28 November 2019 . Published Online: 23 December 2019

Hyeongpin Kim, and Heedeuk Shin

Large on-chip Brillouin net amplification in silicon-based nano-photonics

Cite as: AIP Advances 9, 125032 (2019); doi: 10.1063/1.5125699
Submitted: 25 August 2019 • Accepted: 28 November 2019 •
Published Online: 23 December 2019

Hyeongpin Kim and Heedeuk Shin[a)]

AFFILIATIONS

Department of Physics, Pohang University of Science and Technology (POSTECH), Pohang 37673, South Korea

[a)]Author to whom correspondence should be addressed: heedeukshin@postech.ac.kr

ABSTRACT

Recent developments in on-chip forward Brillouin scattering open up potential applications such as RF photonic signal processing, on-chip Brillouin amplification, and on-chip Brillouin lasers. The stimulated Brillouin scattering gain coefficients become significant with a small optical mode area, and the Brillouin net amplification has been believed to be strong with a small mode area, too. However, here, we present a theoretical study of higher net amplification with a large optical mode area than that with a small mode area and explain this counter-intuitive phenomenon by examining the contribution of various optical forces to Brillouin gain coefficients for various optical waveguide dimensions. The simulation results show that a waveguide with large optical waveguide dimensions can yield significant net amplification by high Brillouin gain coefficients and low optical losses at high pump power even if the Brillouin gain coefficients are lower than that with a small waveguide dimension. Therefore, it is necessary to optimize the optical waveguide dimensions to achieve maximum net amplification for the development of Brillouin lasers and amplifiers in silicon-based nanophotonics.

INTRODUCTION

Large nonlinear optical effects in silicon photonics have been of great interest to the physics and signal processing communities due to their wide range of applications.[1] The stimulated Brillouin scattering (SBS) effect is one of the strongest nonlinear effects in optical fibers, and on-chip SBS effects have been recently observed in silicon waveguides,[2,3] showing great potentials in the applications of on-chip SBS net amplification,[4,5] the SBS laser,[6] efficient microwave signal processing,[7–9] nonreciprocal information amplification,[10] and optomechanical cooling.[11,12]

Subsequent to the demonstration of large forward SBS net amplification in silicon,[4,5] on-chip forward Brillouin gain has been intensively studied in silicon resonators[13,14] achieving high forward SBS gain coefficients; however, the net amplification was not sufficient for an on-chip Brillouin laser. Recently, a silicon Brillouin laser has been demonstrated for the first time using stimulated intermodal Brillouin scattering through a suspended silicon waveguide racetrack structure.[6] It consists of a multimode racetrack cavity with two Brillouin-active regions and a mode-specific coupler. The proposed scheme provides a practical application using forward SBS on a CMOS-compatible silicon chip.

The net amplification in silicon, i.e., larger SBS gain than total optical loss, can be achieved by reducing the optical loss as well as phonon loss. Several types of nano/microphotonic structures have been designed to reduce phonon dissipation through the silica substrate, including phononic crystals,[9,15,16] waveguides supported by pillars,[3] tapered fibers,[17] photonic crystal fibers,[18,19] suspended silicon nanowires,[5] the hybrid (silicon and silicon nitride) Brillouin active membrane (BAM) waveguide with air slots,[2] and the all-silicon BAM waveguide with air slots.[4] The hybrid BAM structure is similar to the all-silicon BAM structure except for the phononic waveguide material, silicon nitride. The hybrid structure using silicon nitride has advantages of tensile stress to support the suspended membrane parts and less the effect from flexural acoustic modes.

Among the various types of on-chip SBS structures, the hybrid BAM waveguide structure investigated in this research has the advantage of independent control of its photonic and phononic waveguides, having more degrees of freedom in designing

structures.[2] The experimental results show a tailorability of the SBS resonant frequency by varying the widths of the phononic waveguides. Moreover, its rich Brillouin resonant features reveal the operational bandwidth of SBS excitation. In Ref. 20, two BAM waveguides with a fixed phononic dimension of 3.8 μm, but with different photonic waveguide widths of 313 nm and 950 nm, were experimentally examined; the results showed that the operational bandwidth is wider with the 313-nm BAM waveguide, but the SBS gain coefficients at low frequencies are comparable to each other. This proved the additional tailorability of the BAM waveguide without significant compromise on the SBS gain. In addition, most of the on-chip SBS experiments have been performed with the smallest optical effective mode area to enhance the Brillouin scattering effects, although it is well known that light in silicon waveguides experiences large linear and nonlinear absorption of silicon such as two-photon absorption (TPA) and TPA-induced free carrier absorption (FCA).[4,21] Thus, the enhancement of on-chip SBS net amplification requires the optimization of both photonic and phononic confinements.

Here, the contributions of electrostrictive (ES) forces and radiation pressure (RP) to the SBS gain coefficients and operation bandwidth are investigated numerically for different optical waveguide dimensions. The results show that the SBS operation bandwidth and gain coefficients have dependence on the width of the photonic waveguide, whereas the fixed phononic waveguide dimensions (slot-to-slot distance) result in nearly constant resonant frequencies. The Brillouin gain coefficient of the fundamental mode has the highest value with the 500-nm width waveguide, but the net amplification is small due to the linear and nonlinear absorption effects on silicon. The powerful on-chip Brillouin net-amplification technologies in silicon nanophotonics can open up a host of wide-band signal processing capabilities and silicon Brillouin lasers.

THEORY AND SIMULATION

A BAM waveguide consists of a silicon waveguide with wings of the silicon nitride membrane on both sides, as shown in Fig. 1, having the advantage of independent control of its photonic and phononic modes. The silicon waveguide at the center of the BAM waveguide guides the photons (the red arrow in Fig. 1), and the silicon nitride wings confine the phonons between the two ends of the wings (white arrows in Fig. 1). The forward SBS process

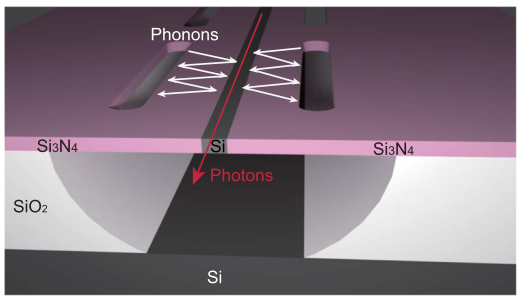

FIG. 1. Photon-phonon interaction through a BAM waveguide, illustrating the propagation directions of optical mode (red arrow) and acoustic waves (white arrows).

requires satisfying both energy-conservation and phase-matching conditions.[18,22,23] The phononic waves travel nearly transversely, satisfying the forward phase matching condition, and tailorable SBS nonlinearities have been demonstrated by varying the silicon nitride wing size while maintaining large SBS gain.[2]

The forward SBS gain coefficients can be numerically calculated using the method of response theory of optical forces as given by[22–24]

$$G_B(\Omega_m) = \frac{\omega Q_m}{2\Omega_m^2 P_p P_s} \frac{\left|\langle \mathbf{f}_{\mathrm{ES}}, \mathbf{u}_{\mathrm{m}} \rangle + \langle \mathbf{f}_{\mathrm{RP}}, \mathbf{u}_{\mathrm{m}} \rangle\right|^2}{\langle \mathbf{u}_{\mathrm{m}}, \rho \mathbf{u}_{\mathrm{m}} \rangle}, \quad (1)$$

where ω is the angular optical frequency of the pump light; P_p (P_s) is the guided power of the pump (Stokes) wave; Ω_m is the frequency of the m-th acoustic mode; $\mathbf{u}_{\mathrm{m}}$ is the displacement of the m-th acoustic mode; ϵ and ρ are the permittivity and density of the corresponding medium, respectively; Q_m is the mechanical Q-factor of the system for the m-th acoustic mode, respectively. Q_m in this study is fixed as 1000. The inner product ($\langle , \rangle$) between the two vector fields signifies the overlap integral over the waveguide cross section.[23] The optical force is induced with the pump light in a silicon waveguide by the electrostrictive force ($\mathbf{f}_{\mathrm{ES}}$) and radiation pressure ($\mathbf{f}_{\mathrm{RP}}$). The ES force occurs due to the change in the shape of a dielectric material under the light of high intensity and can be calculated using the electrostrictive tensor. Radiation pressure (RP) originates from the change of momentum of photons at the boundaries and can be calculated from the Maxwell stress tensor.[22,23] The product of the acoustic displacement of each mode and optical forces determines the SBS gain coefficients represented by $|\langle \mathbf{f}_{\mathrm{ES}}, \mathbf{u}_{\mathrm{m}} \rangle + \langle \mathbf{f}_{\mathrm{RP}}, \mathbf{u}_{\mathrm{m}} \rangle|^2$.

The spectrum of SBS gain coefficients can be optimized by independent control of the BAM structure. The variance in the dimensions of the phononic waveguide affects the acoustic mode displacement, $\mathbf{u}_{\mathrm{m}}$, and resonant frequency, Ω_m. Consequently, multiple resonant frequencies were observed and the adaptability of the SBS resonant frequency over 12 GHz was demonstrated.[2] The photonic waveguide dimension used in Ref. 2 was 313 nm, having fixed optical mode and optical force. With increasing photonic waveguide dimensions, the optical mode area becomes large, yielding smaller optical forces, and the change in the photonic waveguide affects the product of optical forces and acoustic displacement, $\langle \mathbf{f}, \mathbf{u}_{\mathrm{m}} \rangle$. This independent controllability of the optical force and phononic mode must be investigated in depth to achieve large SBS net amplification.

The details of the control of SBS gain coefficients are studied using the three-dimensional finite element method by COMSOL Multiphysics. Figure 2(a) depicts the structure of the BAM waveguide for this simulation. The system consists of a silicon waveguide and two silicon nitride wings with air around them. The air damping effect was neglected in the simulation as the resonant frequency is very high (~GHz) to be affected by air, and the dominant acoustic modes contributing to the SBS gain coefficients are compressive modes in the transverse direction of the silicon waveguide. Other modes such as flexure and shear modes exist in experiments;[2–4] however, they are less effective on the SBS gain coefficients as they do not match well with the transverse optical forces. The thickness of the silicon nitride wings as well as the silicon waveguide is 170 nm to eliminate unwanted flexural and shear modes in the simulation so that only the compressive phononic modes of the wings are considered. The width of the silicon waveguide, b, varies from 250 nm

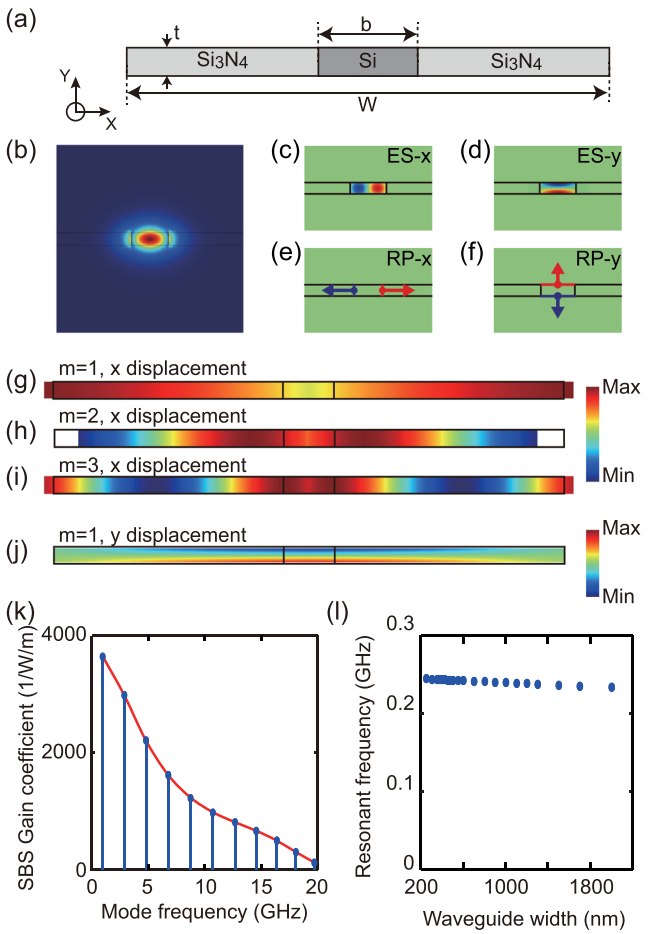

FIG. 2. Computational simulation of forward Brillouin scattering through the BAM waveguide. (a) Cross section of BAM waveguide geometry in the simulation. The silicon waveguide width ***b*** is variable, but the membrane thickness ***t*** is fixed at 170 nm. (b) The computed electric field profile of the fundamental TE-like mode in a BAM waveguide. [(c) and (d)] The computed x- and y-components of the ES force density, respectively. [(e) and (f)] The x- and y-components of the RP-induced boundary forces, respectively. [(g)–(j)] The first three phononic modes of displacement fields in the x-direction identified in (k). (j) The first phononic mode of the y-direction displacement field in (k). Thescale of color bars of (g)–(i) and (j) is 50 times different. (k) SBS gain coefficients (blue circles) of a BAM waveguide with ***W*** = 5 μm and ***b*** = 0.5 μm. The red curve indicates the envelope of allowable SBS gain coefficients under the geometry. (l) The first resonant frequency of a BAM waveguide with ***W*** = 20 μm against the photonic waveguide dimension, ***b***.

to 2000 nm, and the dimension of the phononic mode is W. The mechanical Q-factor in this study is fixed as 1000.

The SBS gain coefficients are estimated numerically by calculating the optical forces from the optical mode and allowable acoustic modes of the BAM system, as shown in Fig. 2(a). The simulation in this study is carried out with the fundamental TE-like modes of the optical system, as shown in Fig. 2(b). The optical wavelength is fixed at 1.55 μm, and the refractive indices of silicon, silicon nitride, and air are 3.48, 1.99, and 1, respectively. For acoustic mode simulation, Poisson's ratio, $[\upsilon_{yz}, \upsilon_{zx}, \upsilon_{xy}] = [0.36, 0.28, 0.064]$, and Young's modulus, $[E_x, E_y, E_z] = [169, 169, 130]$ GPa, were employed.[25] Optical forces were calculated using photoelastic constants $[p_{11}, p_{12}, p_{44}] = [-0.0875, 0.017, -0.051]$.[2,26] The simulation geometry dimensions are $W = 5$ μm and $b = 0.5$ μm. The x-component and y-component of the ES force density calculated from the TE-like mode are shown in Figs. 2(c) and 2(d), respectively. The red (blue) region indicates a region having optical power to the right (left) side in Fig. 2(c) and downward (upward) in Fig. 2(d) at a specific time. Similarly, the x-component and y-component of the RP force density are shown in Figs. 2(e) and 2(f), respectively, indicating that the RP force acts only at the boundaries. The two optical forces yield constructive interference in the x-direction, but the y-component of the ES force is directed opposite to that of the RP, summing up destructively and hindering high SBS gain coefficients. The RP in the y-direction is opposite to the ES force in the y-direction, which can reduce the total SBS gain coefficients slightly; however, its effect is not significant due to much smaller y-displacement than x-displacement.

The acoustic displacement modes induced by the optical forces are shown in Figs. 2(g)–2(j). Figures 2(g)–2(i) present the normalized x-direction displacements of the first three fundamental acoustic modes, and Fig. 2(j) depicts the normalized y-direction displacement of the fundamental acoustic mode. The x-direction displacements are usually two orders of magnitude larger than the y-direction displacements. The simulation result of the SBS gain coefficients is shown in Fig. 2(k), where the red solid curve represents the envelope of the allowable SBS gain coefficients. The SBS gain coefficients decrease at high frequencies, and similar trends are experimentally observed in the data of Refs. 2 and 20. As the most dominant acoustic modes are the compressive modes and the simulation geometry can eliminate the influence of the flexure and shear modes, the envelope of Fig. 2(k) shows a trend similar to the experimental results.[2,20] Figure 2(l) shows the first resonant frequency against the photonic waveguide dimension with $W = 20$ μm. Since the fixed phononic waveguide dimension with varying photonic waveguide dimension yields a small change, less than 5%, we neglect this variance in this study.

RESULTS

The operation bandwidth due to the SBS effect is examined for various photonic waveguide widths $b = [250, 300, 500, 1000, 2000]$ nm with a fixed phononic waveguide dimension of 20 μm. Here, we present the result for a wing width $W = 20$ μm, as the wing width does not affect the trend of the envelopes. From the calculated SBS gain coefficients, the envelopes of the normalized SBS gain coefficients contributed by both ES and RP are shown in Fig. 3(a). The envelopes in Fig. 3(a) clearly indicate that the bandwidths of the envelopes become narrower with a decrease in the dimensions of the optical waveguide. By controlling only the optical waveguide, the spectrum of SBS gain coefficients can be specifically designed. The SBS gain coefficients decrease at higher frequencies mainly due to the effect of Ω_m^2 in Eq. (1); therefore, with the same amount of work by the optical forces, the SBS gain coefficient of the fundamental mode is higher than that of the higher modes. From the results of the SBS envelopes in Fig. 3(a), we define the excitation bandwidth as the frequency at half maximum of the envelopes. In order to explain the behavior of excitation bandwidth simply, we simplify Eq. (1) with $|\langle \mathbf{f}_{ES}, \mathbf{u}_m \rangle + \langle \mathbf{f}_{RP}, \mathbf{u}_m \rangle|^2 \propto |\mathbf{u}_m|^2 |\boldsymbol{E}|^4 A^2$, $P_p P_s \propto |\boldsymbol{E}|^4 A^2$

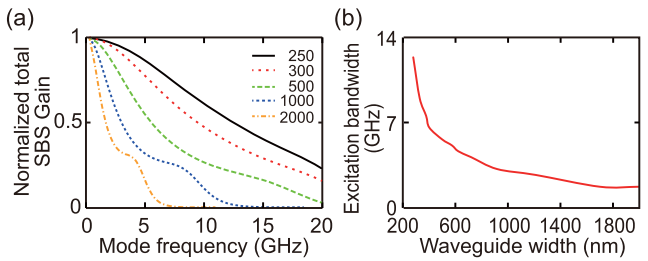

FIG. 3. Simulated Brillouin scattering gain coefficient envelope through BAM waveguides. (a) Envelope of SBS gain coefficients for various photonic waveguide widths ***b*** = [250, 300, 500, 1000, 2000] nm. The phononic waveguide dimension and thickness of the BAM waveguide are fixed at ***W*** = 20 μm and ***t*** = 170 nm, respectively. SBS coefficients are calculated using both ES and RP forces. (b) Excitation bandwidth of calculated SBS gain coefficients for photonic waveguide widths ***b***.

and $\langle \mathbf{u}_m, \rho \mathbf{u}_m \rangle \propto \epsilon |\mathbf{u}_m|^2 A$. Therefore, $G_B(\Omega) \propto \frac{1}{A\Omega_m^2}$, when Q_m is fixed. If the SBS gain coefficient is normalized, then the excitation bandwidth is inversely proportional to the square root of the waveguide cross-sectional area A, $\Omega_{m,half} \propto \frac{1}{A^{1/2}}$. The realistic situation is more complicated, but the simplified relationship of Eq. (1) reveals the reduction of the excitation bandwidth. As shownin Fig. 3(b), the calculated excitation bandwidth decreases significantly with the increase in the width of the waveguide due to the overlap between the optical and acoustic modes.

Next, we investigate the contribution of the individual ES force and RP to the total SBS gain coefficients. The SBS gain coefficient of the first Brillouin mode (G_{1st}) that is contributed by RP, ES force, and both RP and ES forces is shown in Fig. 4(a) for the photonic

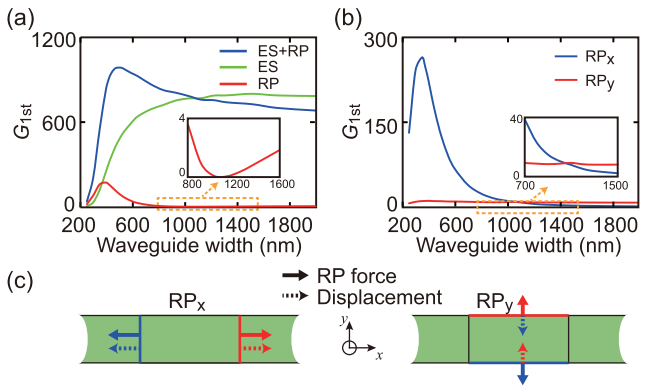

FIG. 4. SBS gain coefficients by optical forces. (a) SBS gain coefficients of the fundamental phononic modes for photonic waveguide widths ***b***. The fundamental gain coefficients contributed by both ES and RP forces (blue), ES forces only (green), and RP forces only (red). The inset shows the point where ES and RP interfere destructively with each other. (b) Work done by the x-component (blue) and y-component (red) of RP for varying photonic waveguide widths ***b***. (c) Direction of x- and y-components of RP and displacement. The solid lines display the direction of RP force, and the dotted lines indicate the direction of displacement. The structure on the simulation is 20 μm of the phononic waveguide dimension (***W***) and 170 nm of thickness (***t***).

waveguide width b. The blue solid curve shows the SBS gain coefficient of the fundamental mode induced by both the ES force and RP, and the green (red) line indicates the SBS gain coefficient by the ES force (RP) individually. At small b, the contribution of RP to the SBS gain coefficient (red) exceeds that of the ES force (green); however, it decreases significantly at large b due to a reduction in the electric field and its discontinuity at the boundaries between the silicon waveguide and silicon nitride membrane. In contrast to the trend of the contribution of RP, the contribution of the ES force (green) increases at higher b as the overlap between the optical and acoustic modes increases, inducing a large contribution of the ES force to the SBS gain coefficient. As the total SBS gain coefficient is proportional to $|\langle \mathbf{f}_{ES}, \mathbf{u}_m \rangle + \langle \mathbf{f}_{RP}, \mathbf{u}_m \rangle|^2$, the total SBS gain coefficient (blue) has the maximum value at an approximate value of b = 500 nm.

The SBS gain coefficients are large for small photonic mode areas as the optical mode with a small core yields strong optical forces by ES and RP. The simulation results show that the Brillouin gain coefficient through the BAM waveguide has the largest value at a waveguide width of 500 nm, as shown in Fig. 2(a). The Brillouin active nonlinearities with a narrow silicon waveguide can be observed over a wide range of frequencies (>10 GHz), having a wide operation bandwidth. The compact confinement of the optical mode in the silicon waveguide allows for this wide operation bandwidth with large Brillouin gain coefficients due to strong optical forces.

The SBS by RP in the inset of Fig. 4(a) has null gain coefficients at a width of approximately 1000 nm, and the total SBS gain coefficients at widths over 1000 nm are less than that by only the ES, as shown in Fig. 4(a), indicating that the two optical forces of ES and RP interfere destructively. To analyze this phenomenon, the SBS gain coefficients contributed by RP are investigated in detail by separating the contributions of the x- and y-components of RP, as shown in Fig. 4(b). The SBS gain coefficients by the x-component of RP (blue curve) are maximum at a width of nearly 400 nm and decrease for large dimensions as the electric field is mostly confined at the center of the waveguide and the discontinuity of its tail at the boundary is weakened. Moreover, as the thickness of the waveguide is fixed, the strength of the y-component of RP (red curve) is constant, as shown in Fig. 4(b). If the width of the waveguide is more than 1000 nm, the y-component of the RP optical force exceeds the x-component, as shown in the inset of Fig. 4(b). Finally, by considering the directions of the RP force and displacement, the destructive interference in Fig. 4(a) can be explained. The x-directional displacement and RP work in the same direction as shown in Fig. 4(c), but the y-directional displacement is opposite in direction with respect to that of RP. In Eq. (1), this opposite direction of displacement causes the destructive interference for waveguides of widths over 1000 nm.

The SBS gain represents the photon energy transferred from the pump beam scattered by the acoustic wave. If the length of the BAM waveguide is L, then the SBS gain is defined as $\left| \frac{A_{stokes}(L, \omega_p - \omega_s = \Omega_m)}{A_{stokes}(L, \omega_p - \omega_s = \Omega_m + \Delta\Omega)} \right|^2$, where $\Delta\Omega$ is the detuning frequency from the resonant frequency much larger than the SBS gain bandwidth and A_{Stokes} is the amplitude of the Stokes optical mode. In other words, the SBS gain is defined as the ratio of the transmitted Stokes power at a resonant frequency to that at a nonresonant frequency. It indicates the strength of the SBS effect, but not the amplification of light. The net amplification is the power ratio between the input and output powers of a BAM waveguide at the resonant frequency,

considering both the SBS gain and waveguide loss. The net amplification is defined as $\left|\frac{A_{stokes}(L,\omega_p-\omega_s=\Omega_m)}{A_{stokes}(0,\omega_p-\omega_s=\Omega_m)}\right|^2$. It is a parameter exhibiting the usefulness of a system for applications such as lasers and amplifiers. To simulate net amplification, the optical power generated through a BAM waveguide is numerically calculated using both the SBS gain of the simulations and typical linear and nonlinear losses of the silicon waveguide. The pump and Stokes light power can be expressed in small signal limits as[4,21]

$$\frac{1}{P_p(z)}\frac{dP_p(z)}{dz} = -\left(\alpha_0 + \beta P_p(z) + \gamma P_p^2(z)\right), \quad (2)$$

$$\frac{1}{P_s(z)}\frac{dP_s(z)}{dz} = -\alpha_0 + (G_B(\Omega_m) - 2\beta - \gamma P_p(z))P_p(z), \quad (3)$$

where $P_p(z)$ and $P_s(z)$ are the intensities of the pump and Stokes signal at position z, respectively, and $G_B(\Omega_m)$ are the SBS gain coefficients at the resonant frequency. α_0, β, and γ are the linear, two-photon absorption (TPA), and TPA-induced free carrier absorption (FCA) coefficients, respectively. The linear loss coefficient is inversely proportional to the fourth power of the optical waveguide width ($\alpha_0 = A \times b^{-4} + B$) as the loss due to the scattering effects on the side walls decreases with increasing width of the waveguide.[27] The constants A = 0.578 μm^4/m and B = 19.86/m are chosen from the experimental results in Ref. 20 (α_0 = 7 dB/cm for b = 313 nm and α_0 = 1 dB/cm for b = 950 nm). In addition, the TPA and FCA coefficients depend on the bulk parameters of silicon and the effective mode area (A_{eff}) of the fundamental optical mode as $\beta = 5 \times 10^{-12}/A_{eff}\ m^{-1}\ W^{-1}$ and $\gamma = 5.65 \times 10^{-23}/A_{eff}^2\ m^{-1}\ W^{-2}$.[28]

The small mode area of a silicon waveguide can induce not only large SBS gain coefficients but also large nonlinear absorptions by TPA and FCA,[23] resulting in shorter effective propagation length and lower power handling of the system. Moreover, the FCA loss becomes significant at high intensities as it is a fifth order nonlinear effect. Figure 5 shows the net amplification through a 1-cm long BAM waveguide for input pump powers of $P_p(0)$ = [0.01, 0.1, 0.3, 0.7] W. The net amplification of a BAM waveguide with $W = 20\ \mu m$ is numerically calculated using a mechanical Q-factor of 1000 of the phononic system. At a width of approximately 500 nm, the SBS gain coefficient in Fig. 4(a) attains a maximum value, although the net amplification is low with high pump power. The effective mode area of an electric field, as shown in the inset of Fig. 5, has the smallest value at nearly 500 nm inducing high nonlinear losses, especially FCA,[29] which is proportional to the square of the pump power. Consequently, due to the less compact optical confinement in wider waveguides and low nonlinear absorption, the net amplification for a 2-μm-wide waveguide is higher than that in narrower waveguides.

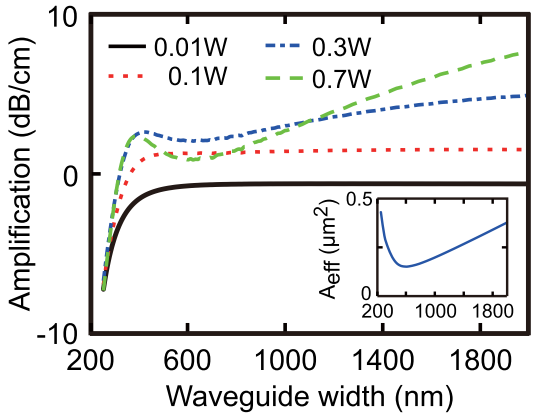

FIG. 5. Simulated net amplification per unit length through the BAM waveguide. Net amplification per cm for pump powers of $\boldsymbol{P_p}(0)$ = [0.01, 0.1, 0.3, 0.7] **W** for waveguide widths with phononic dimension $\boldsymbol{W}$ = 20 μm. Inset: Calculated effective mode areas of BAM waveguides of the fundamental SBS mode for waveguide widths ***b***.

DISCUSSION

In our main results about the excitation bandwidth, SBS gain coefficients, and net amplification, phononic waveguide dimension W is fixed at 20 μm. Because the change of W mainly affects the integral domain of denominator of Eq. (1), large (small) phononic dimension reduces (enhances) SBS gain coefficients, but it does not change the trends of our main results. We discuss the SBS effects only in the BAM waveguide geometry, but the SBS gain coefficient calculations are based on the electrostriction and radiation pressure effects,[22] which participate in Brillouin scattering not only in the BAM waveguide but also in other structures. Therefore, these results can be applied in other structures.

Dimensional inhomogeneity and asymmetric structural shape can lead to broadening the Brillouin resonance and reducing the Q-factor and then decreasing the SBS gain.[30] The geometry with an even membrane thickness of 170 nm as in Fig. 2(a) can induce high mechanical Q-factors of the system due to its symmetric structure. In Ref. 2, the geometry is similar to that in this study and the measured Q-factor values are over 1800. The measured Q-factor values in Ref. 4 are, however, smaller than those in Ref. 2 due to the geometry and inhomogeneity caused by the fabrication imperfection. Therefore, we believe that it is reasonable to use a Q-factor value of 1000 in this study. Various geometries or dimensions including thickness, wing size, and length will also induce varied resonant frequencies and Q-factors. Further study about the relation between geometry and Q-factor is required. The net amplification in Fig. 5 may vary with reduced SBS gains by the fabrication imperfection or geometry, but the fact that wide photonic waveguide widths are appropriate to obtain high Brillouin net amplification will not change. This behavior will be significant when the pump power is high in a resonator such as the Brillouin laser.

In this paper, we study the SBS excitation bandwidth and net amplification in the BAM waveguide structure. The excitation bandwidth, the bandwidth of the acoustic harmonics, decreases inversely proportionally to the cross-sectional area of the photonic waveguide dimension. In addition, the electrostriction effects increase as the waveguide dimension increases, but the radiation pressure effects are maximized with about 400-nm photonic waveguide width and decrease due to the confliction between the horizontal and vertical radiation pressure components. By combining these two effects, the SBS gain coefficients will have the maximum value with about 500-nm waveguide width. The net amplification, however, shows different trends due to the nonlinear losses in silicon. As the nonlinear losses depend on the intensity (optical power divided by the mode area), a large waveguide dimension is recommended in order

to achieve high amplification in high optical power. This behavior will be a significant factor in designing an on-chip Brillouin amplifier and Brillouin laser.

ACKNOWLEDGMENTS

This work was supported by the National Research Foundation of Korea (NRF) (Grant No. NRF-2017R1C1B2011113).

REFERENCES

[1]Q. Lin, O. J. Painter, and G. P. Agrawal, Opt. Express **15**, 16604 (2007).
[2]H. Shin, W. Qiu, R. Jarecki, J. A. Cox, R. H. Olsson, A. Starbuck, Z. Wang, and P. T. Rakich, Nat. Commun. **4**, 1944 (2013).
[3]R. Van Laer, B. Kuyken, D. Van Thourhout, and R. Baets, Nat. Photonics **9**, 199 (2015).
[4]E. A. Kittlaus, H. Shin, and P. T. Rakich, Nat. Photonics **10**, 463 (2016).
[5]R. Van Laer, A. Bazin, B. Kuyken, R. Baets, and D. Van Thourhout, New J. Phys. **17**, 115005 (2015).
[6]N. T. Otterstrom, R. O. Behunin, E. A. Kittlaus, Z. Wang, and P. T. Rakich, Science **360**, 1113 (2018).
[7]D. Marpaung, B. Morrison, M. Pagani, R. Pant, D.-Y. Choi, B. Luther-Davies, S. J. Madden, and B. J. Eggleton, Optica **2**, 76 (2015).
[8]L. McKay, M. Merklein, A. C. Bedoya, A. Choudhary, Y. Liu, M. Jenkins, C. Middleton, A. Cramer, J. Devenport, A. Klee, R. DeSalvo, and B. J. Eggleton, Optica **6**, 907 (2019).
[9]H. Shin, J. A. Cox, R. Jarecki, A. Starbuck, Z. Wang, and P. T. Rakich, Nat. Commun. **6**, 6427 (2015).
[10]N. T. Otterstrom, E. A. Kittlaus, S. Gertler, R. O. Behunin, A. L. Lentine, and P. T. Rakich, Optica **6**, 1117 (2019).
[11]N. T. Otterstrom, R. O. Behunin, E. A. Kittlaus, and P. T. Rakich, Phys. Rev. X **8**, 041034 (2018).
[12]G. Bahl, M. Tomes, F. Marquardt, and T. Carmon, Nat. Phys. **8**, 203 (2012).
[13]R. Zhang, J. Sun, G. Chen, M. Cheng, and J. Jiang, Appl. Phys. Lett. **111**, 031102 (2017).
[14]Y. Zhang, L. Wang, Z. Cheng, and H. K. Tsang, Appl. Phys. Lett. **111**, 041104 (2017).
[15]R. Zhang, G. Chen, and J. Sun, Opt. Express **24**, 13051 (2016).
[16]R. Zhang and J. Sun, J. Lightwave Technol. **35**, 2917 (2017).
[17]M. S. Kang, A. Brenn, G. S. Wiederhecker, and P. S. J. Russell, "Stimulated brillouin scattering and applications," in *Conference on Lasers and Electro-Optics (CLEO)* (San Jose, CA, 2008), CTuB5.
[18]M. S. Kang, A. Nazarkin, A. Brenn, and P. S. J. Russell, Nat. Phys. **5**, 276 (2009).
[19]W. H. Renninger, H. Shin, R. O. Behunin, P. Kharel, E. A. Kittlaus, and P. T. Rakich, New J. Phys. **18**, 025008 (2016).
[20]H. Shin, J. A. Cox, R. Jarecki, A. Starbuck, W. Qiu, Z. Wang, and P. T. Rakich, in *Frontiers in Optics* (Tucson, AZ, 2014), FW4B.3.
[21]M. J. Steel, B. J. Eggleton, P. Gutsche, C. Wolff, and C. G. Poulton, J. Opt. Soc. Am. B **32**, 1968 (2015).
[22]P. T. Rakich, C. Reinke, R. Camacho, P. Davids, and Z. Wang, Phys. Rev. X **2**, 011008 (2012).
[23]W. Qiu, P. T. Rakich, H. Shin, H. Dong, M. Soljačić, and Z. Wang, Opt. Express **21**, 31402 (2013).
[24]P. T. Rakich, M. A. Popović, and Z. Wang, Opt. Express **17**, 18116 (2009).
[25]M. A. Hopcroft, W. D. Nix, and T. W. Kenny, J. Microelectromech. Syst. **19**, 229 (2010).
[26]L. S. Hounsome, R. Jones, M. J. Shaw, and P. R. Briddon, Phys. Status Solidi A **203**, 3088 (2006).
[27]K. K. Lee, D. R. Lim, H. C. Luan, A. Agarwal, J. Foresi, and L. C. Kimerling, Appl. Phys. Lett. **77**, 1617 (2000).
[28]R. Dekker, N. Usechak, M. Först, and A. Driessen, J. Phys. D: Appl. Phys. **40**, R249 (2007).
[29]J. Leuthold, C. Koos, and W. Freude, Nat. Photonics **4**, 535 (2010).
[30]C. Wolff, R. Van Laer, M. J. Steel, B. J. Eggleton, and C. G. Poulton, New J. Phys. **18**, 025006 (2016).